Research Article Vol. 38, No. 8 / August 2021 / Journal of the Optical Society of America B B35

Journal of the Optical Society of America B

OPTICAL PHYSICS

Stimulating polarization switching dynamics in mid-infrared quantum cascade lasers

Olivier Spitz,[1,*] Andreas Herdt,[2] Wolfgang Elsässer,[2] and Frédéric Grillot[1,3]

[1]LTCI, Télécom Paris, Institut Polytechnique de Paris, 19 Place Marguerite Perey, Palaiseau 91120, France
[2]Technische Universität Darmstadt, Schlossgartenstraße 7, D-64289 Darmstadt, Germany
[3]Center for High Technology Materials, University of New Mexico, 1313 Goddard SE, Albuquerque, New Mexico 87106, USA
*Corresponding author: olivier.spitz@telecom-paris.fr

Received 15 March 2021; revised 18 June 2021; accepted 18 June 2021; posted 21 June 2021 (Doc. ID 425097); published 14 July 2021

A unique feature of quantum cascade lasers relies on the ultrafast carrier relaxation lifetime that occurs on a picosecond time scale. Furthermore, the very sharp electronic transitions among the conduction-band states (subbands) lead to specific selection rules, which in theory exclude the TE-polarized light emission. Under cross-polarization reinjection, we stimulate the polarization switching dynamics in such an intersubband device. The mid-infrared modulation signal is phase-shifted between the TM mode and the TE mode, with a typical microsecond time scale different from pure time-delay dynamics. We also prove that both the frequency and the duty cycle of the modulated pattern can be slightly tuned by varying the characteristics of the reinjected light. These results reveal the possibility of favoring the TE polarization in a quantum cascade laser and generating a square-wave modulation with cross-polarization reinjection.

https://doi.org/10.1364/JOSAB.425097

1. INTRODUCTION

Semiconductor lasers usually emit linearly polarized light due to the symmetry of their gain medium and their inherent material anisotropy. This is typically the case for optical sources relying on intersubband transitions [1] because only the component of the electric field normal to the quantum wells can optically couple to the quantum oscillators, which results from quantization of the allowed displacement. The parallel components are left to interact weakly with a free two-dimensional electron gas. For a symmetric quantum well, the ratio $\bar{r}$ between the two orthogonal components of the electric field is given by [2]

$$\bar{r} = \zeta \frac{(E_{n'} - E_n)\Delta_0}{(E_n + E_g + \Delta_0)(E_{n'} + E_g)}, \tag{1}$$

with $\zeta < 1$ a constant coefficient depending on the subband index difference parity, $(E_{n'} - E_n)$ the energy separation between bands, Δ_0 the spin-orbit splitting, and E_g the fundamental energy gap of the material. Typical theoretical values are around 1% and are in good agreement with experimental studies [3]. For instance, quantum cascade lasers (QCLs) emit a wave that is mostly TM-polarized, even if recent efforts showed it is not perfectly linearly polarized, and more specifically, for distributed feedback QCLs [4]. In the case of QCLs, it is possible to implement waveguide polarization mode converters leading to a fixed value of the TE polarization fraction, which can amount up to 70% [5]. However, this method is not useful for high-speed polarization switching.

The technique of feeding back a rotated polarization to a laser [6], known as cross-polarization reinjection, has proved its ability to rotate the polarization of the light emitted by a semiconductor laser [7]. Numerical and experimental efforts carried out on standard interband laser diodes showed that these lasers do not only display a chaotic behavior [8], which is usual with conventional optical feedback and phase-conjugate feedback [9], but can also emit a train of square waves, with sometimes a tuning of the duty cycle depending on the injection strength [10]. The peculiarity of this square wave is that it is simultaneously present in the TE mode and in the TM mode, with a phase shift, and that the upper part of the square wave can exhibit fast oscillations beyond the relaxation frequency of the laser diode, provided that the feedback strength is large enough [11]. Like other nonlinear dynamics found in semiconductor lasers, such as extreme pulses [12] or chaotic oscillations [13], polarization switching can be detrimental in optical metrology or communication because it disturbs the stable signal of the laser. However, the adequate control of such nonlinear dynamics was proven useful for various applications, e.g., private communication [14] or chaotic lidar [15]. In the case of polarization switching, optical routing [16], clock recovery [17], and random number generation [18] have already been reported.

When applying conventional optical feedback to a QCL, the back-reflected wave is mainly TM-polarized, and this triggers nonlinear dynamics in the TM mode of the laser [19]. Yet, this work shows an experimental technique to stimulate the residual TE emission of a QCL by applying a cross-polarization

reinjection technique. The resulting wave is a square-wave modulation with a characteristic time in the order of hundreds of nanoseconds, a rise time of a few dozens of nanoseconds, and a phase shift between the TE wave and the TM wave. It is relevant to note that the state-of-the-art experimental efforts with mid-infrared external modulators manage to produce square patterns with similar characteristics [20].

2. EXPERIMENT

In order to confirm that what we observe is not related to defects in a given laser, we perform the experiment on two different QCLs. One is a Fabry–Perot (FP) QCL emitting around 4.0 μm and housed in a high heat-load (HHL) package (Fig. 1, top inset). The other one is a distributed feedback (DFB) QCL emitting at 5.67 μm and mounted in a Newport LDM-4872 socket (Fig. 1, main picture and bottom inset). This DFB laser emits single-mode radiation with 30 dB side-mode suppression. The device was grown by molecular beam epitaxy on an InP cladding and incorporates 30 periods of AlInAs/GaInAs layers [21]. The upper InP cladding is n-doped at a value of 10^{17} cm^{-3} in order to get electrical injection but without introducing any plasmonic effects. The design uses index coupling and metal grating [22]. This enables single-mode emission using a top metal grating with a coupling efficiency of $\kappa \approx 4\ cm^{-1}$. The QCLs emit continuous wave thanks to a standard double trench configuration without iron-doped indium phosphide regrowth for thermal heat sinking optimization. The back facet of this laser is composed of a high-reflectivity coating, and this means that the laser only generates mid-infrared light at one side that is left as-cleaved. This emitting facet has a transmission of 30% that is suitable for feedback experiments. The waveguide is 14 μm-wide and 2 mm-long. The FP-QCL is a commercial model from Alpes Lasers, and we do not have access to its material properties. However, choosing two QCLs with many differences in terms of structure confirms that the phenomenon we observed is not related to defects in a given structure.

The QCL under study is placed in an external optical feedback configuration with cross-polarization reinjection. The back-reflected light is rotated from a mostly TM-polarized radiation to a mixed TE/TM wave with a quarter-wave plate (QWP) with angle ψ; the characterization of the light sent back to the laser is given in Fig. 2. The whole setup is visualized in Fig. 3. A first nonpolarizing beam splitter (NPBS1) divides the light

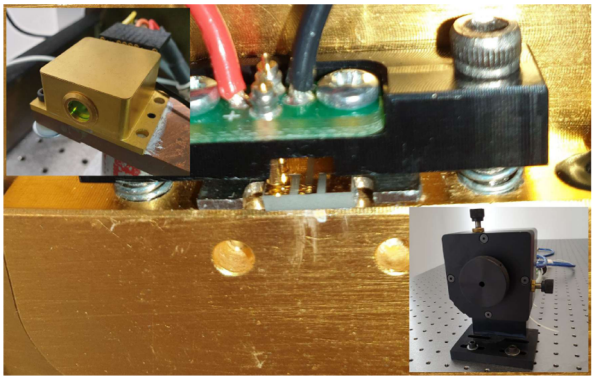

Fig. 1. QCL embedded in a LDM-4872 mount (center) and global picture of the two different mounts used in this experiment (insets).

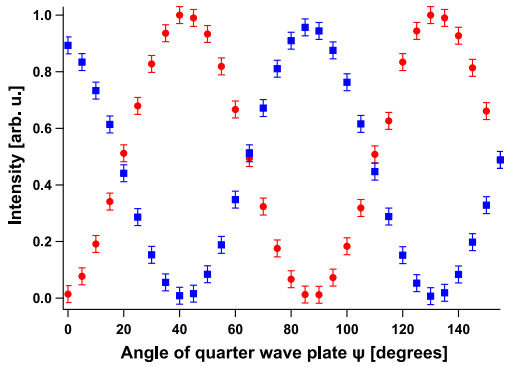

Fig. 2. Characterization of the TE light (circles) and the TM light (squares) that are reinjected into the QCL after one round trip in the external cavity with the QWP.

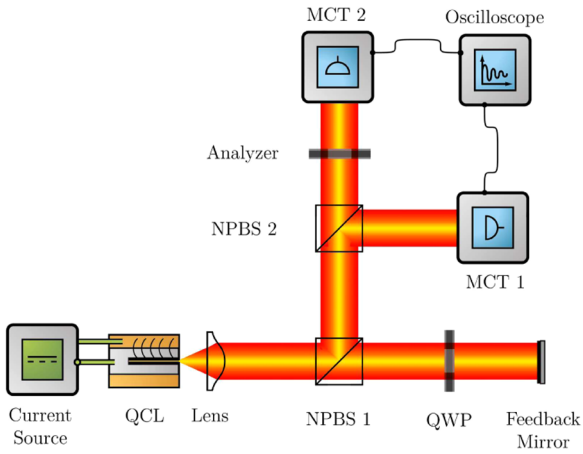

Fig. 3. Experimental setup for cross-polarization reinjection, which differs from conventional optical feedback schemes because of the QWP inside the external cavity. MCT, mercury-cadmium-telluride detector; NPBS, nonpolarizing beam splitter.

between the external cavity and the analysis branch. The light is subsequently split by a second beam splitter (NPBS2) between the first mercury-cadmium-telluride detector (MCT1), which acts as a reference-signal detector for phase-shift measurements, and the second detector (MCT2), preceded by an analyzer with angle θ to detect either the TE ($\theta = 0°$) or the TM radiation ($\theta = 90°$). NPBS1 has a very high transmission of 70%, and this allows for strong feedback strength.

With our setup, it is possible to precisely determine the phase shift between the TM mode and the TE mode that we are able to excite. The TM time trace detected by MCT2 is compared with the reference signal (unfiltered QCL signal) detected by MCT1. The same goes for the TE time trace, and the only difference is the value of θ, the angle of the analyzer. Figures 4(a) and 4(b) show the original files where the reference signal is displayed simultaneously with the TM signal and the TE signal, respectively. The reference signal is actually the direct output signal of the QCL, so it should look very similar to the TM signal, as we will see that the QCL's signal remains mainly TM-polarized. However, the electrical bandwidth of this detector (MCT1) is not designed for the frequencies we study. Consequently, the reference signal looks distorted, but what matters for the

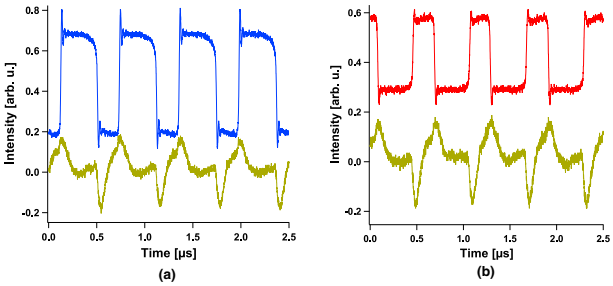

Fig. 4. Experimental wave emitted by the DFB-QCL under study when cross-polarization reinjection is applied for a QWP at 35° and when (a) the analyzer is set to 90° for TM-mode display; (b) the analyzer is set to 0° for TE-mode display. The (a) top waveform corresponds to the TM wave, the (b) top waveform corresponds to the TE wave and the bottom waveforms correspond to the reference signal. Time traces are initially centered around zero, but they are vertically shifted for clarity.

reference is the repetition rate, and that is clearly visible in the gold time trace. With these two reference charts, the phase shift between the TM signal emitted by the QCL and the TE signal can be identified, and the combination of these two time traces allows printing Fig. 5(b).

3. RESULTS

One of the key experimental parameters is the angle ψ of the QWP. When the QWP is set to 45°, we observe a square pattern for the TM mode and for the TE mode, with a phase shift between the two, as shown in Fig. 5(a). This is very similar to what was reported for laser diodes and vertical-cavity surface-emitting lasers (VCSELs) [11,23]. However with QCLs, the period of the square pattern is not related to that of the external cavity, as previously observed in semiconductor lasers. In our case, the external cavity round-trip time is 2.4 ns, whereas the period of the square pattern is in the order of 500 ns. Because we are not in a configuration with a Faraday rotator, multiple beam reflections can occur within the external cavity, and this would lead to nonlinear dynamics with periods longer than that of a single round-trip time. Nevertheless, this possibility is very unlikely in our case because this would imply that what we observe is a pattern linked to, roughly, 200 round trips within the external cavity. Furthermore, it is possible to slightly tune the frequency of the square-wave signal when varying the angle of the QWP. Changing ψ can also modify the ratio between the TE mode and the TM mode while maintaining the square pattern. When $\psi = 35°$, the square pattern is split between the TM mode for 65% of the time and the TE mode for 35% of the time, the two modes remaining phase-shifted as shown in Fig. 5(b). This behavior has already been observed in the case of coupled laser diodes and was attributed to a change in the coupling strength [24]. In our case, varying the value of ψ from 45° to 35° induces a reduction of the TE reinjection in the QCL, as shown in Fig. 2, and this could be compared with the aforementioned configuration with near-infrared lasers. Because we do not use a Faraday rotator, it is not possible to tune the amount of backreflected TE light when the angle ψ is fixed: any subsequent polarizer or attenuator on the way back to the QCL cavity would affect the intensity of the light that is primarily emitted by the QCL. When ψ is further decreased below 35°, the square pattern disappears because the TE feedback strength is too low. Similar behaviors have been reported in near-infrared semiconductor lasers where only very strong cross-polarization reinjection leads to square-wave emission [11].

Even if the length of the external cavity were not changed, the period of the pattern is changed when varying the value of ψ from 45° to 35°. It is relevant to note that in the two aforementioned cases ($\psi = 45°$ and $\psi = 35°$), no oscillations were spotted on top of the square pattern, as reported in some recent experiments with VCSELs [11]. The lack of such oscillations in our experiment with QCLs can be explained either by the nonexistence of relaxation frequency in QCLs [25], by the limited bandwidth of the mid-infrared detector we used (estimated 3-dB bandwidth of 700 MHz per manufacturer's specifications), or by the fixed value of the feedback strength when ψ is fixed. The characteristic time in the order of microseconds

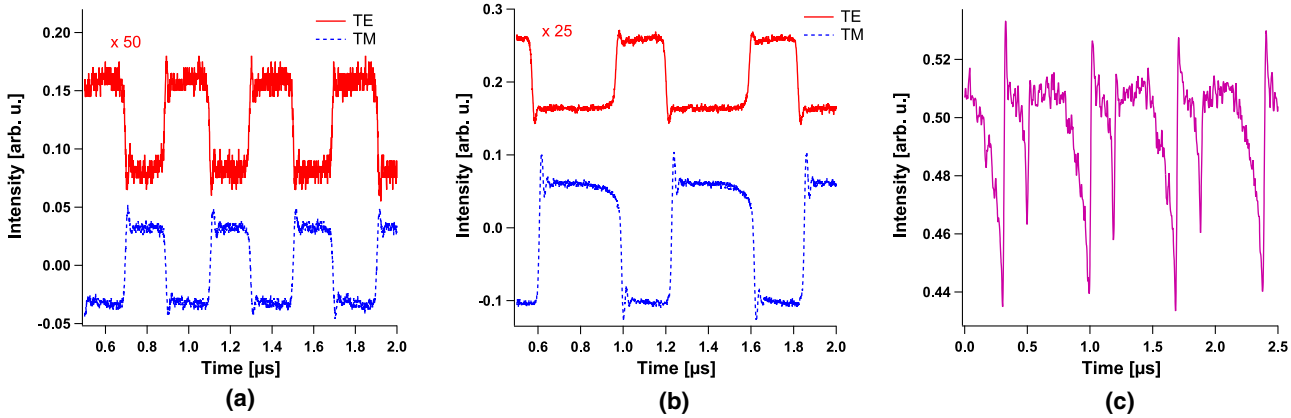

Fig. 5. (a) Experimental time traces of the wave emitted by the DFB-QCL under study when cross-polarization reinjection is applied and the QWP is set to 45°. The bottom dashed waveform corresponds to the TM wave, the top solid line waveform corresponds to the TE wave, and the duty cycle in both cases is close to 50%. (b) Same configuration, but for a QWP set to 35°. In this case, the TM wave has a duty cycle of 65%, while the TE wave has a duty cycle of 35%. For these two charts, the amplitude of the TE mode is magnified to be comparable with that of the TM mode. (c) Response of the detector when $\theta = 10°$, showing both modulated modes with similar amplitude. Time traces are initially centered around zero, but they are vertically shifted for clarity.

confirms that the TE phenomenon is not a backreflection artifact, since the external cavity round-trip time is only a few nanoseconds. Consequently, the observed phenomenon cannot be only attributed to pure time-delay destabilization. This kind of behavior has already been observed in quantum-dot lasers under optical injection [26] and was supported by a Van der Pol–FitzHugh–Nagumo model [27]. This model consists in a general scenario of relaxation oscillations, which are characterized by the competition of two time scales: the time scale of carriers in the nanosecond range and a thermal time scale in the microsecond range. However, this model requires the system to oscillate around a bifurcation point, and this may not be the case for our experiment with a QCL pumped largely above the current threshold. Yet, QCL are semiconductor lasers requiring large pumping current, and a peculiar thermal contribution could play a role in triggering dynamics in the megahertz range. This hypothesis could also explain the large difference when deriving the linewidth enhancement factor of QCLs with low-frequency and high-frequency methods [28]. In coupled laser-diode systems, the predominant role of noise has also been underlined, especially in the asymmetric square-wave case [24], and further investigation is required to explain the long time-scale behavior in QCLs.

In order to measure the ratio between the dynamics of the TE and the TM modes, we tilt θ, the angle of the analyzer, so that both signals are displayed in the same time trace and with comparable amplitudes, as illustrated in Fig. 5(c). By assessing their respective intensity, it is possible to derive the following relationship:

$$\frac{A_E}{A_M} = \frac{\cos^2(90-\theta)}{C \times \cos^2(\theta)}, \tag{2}$$

where $\frac{A_E}{A_M}$ is the ratio between the dynamics of the TE and the TM modes; and C is the ratio between the amplitude of the two square components in a given time trace. In the case where $\theta = 10°$, both squares have nearly the same amplitude, which corresponds to $C = 1$. Thus $\frac{A_E}{A_M} = 3\% \pm 1\%$. It is worth noting that the average output power of the TE mode of the free-running QCL is less than 0.4 % of the TM mode when measured with a power meter. Indeed, if MCT2 is replaced by a thermopile sensor, the output power of the QCL is 54 mW when $\theta = 90°$ (TM light) while the power meter indicates roughly 200 μW, which is the minimum detectable power, when $\theta = 0°$ (TE light). Consequently, the amplitude of the modulated signal in both modes cannot be related to the mean output power when the laser is not subject to any optical feedback.

In the case of the FP-QCL, the same phenomenon is observed with a phase shift between the TM mode and the TE mode and a typical period in the order of 1 μs, different from the external cavity period. The only difference with the DFB-laser configuration is that the periodic pattern we retrieve is not exactly square-like, as can be visualized in Fig. 6. This change in nonlinear dynamics shape has already been numerically observed in other semiconductor structures [10]. The fact that we are able to generate polarization-switching dynamics in two different QCLs shows that the phenomenon we observe is not related to the Bragg grating associated with the DFB laser under study but

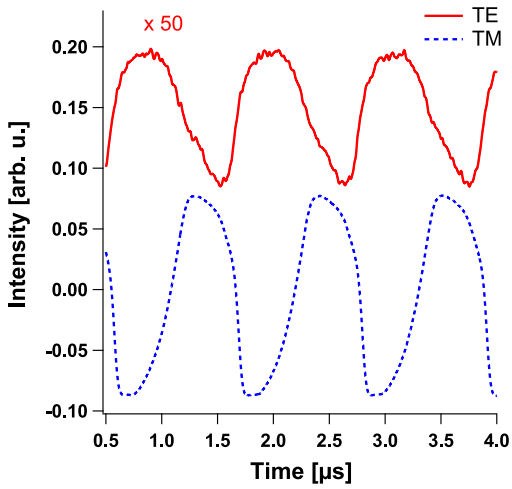

Fig. 6. Experimental time traces of the wave emitted by the FP-QCL under study when cross-polarization reinjection is applied and the QWP is set to 45°. The bottom dashed waveform corresponds to the TM wave, and the top solid line waveform corresponds to the TE wave. The amplitude of the TE mode is magnified to be comparable with that of the TM mode. Time traces are initially centered around zero, but they are vertically shifted for clarity.

to the intersubband structure of the QCL itself. In the FP-QCL configuration, the dynamics amplitude ratio $\frac{A_E}{A_M}$ is also in the order of a few percent, while the ratio between the TE mode and the TM mode remains below 0.6 % when the QCL is free-running. The latter value is a bit higher than in the DFB-QCL configuration because our FP-QCL generates less power in free-running operation, while the minimum detectable power with the thermopile sensor remains unchanged. As a final remark, it is relevant to note that the MCT detectors we used in this experiment have a DC output, but they behave as a low-pass filter with a cutoff frequency well below 1 MHz. It was thus not possible to compare the mean power of the QCL with the amplitude of the square patterns in TM mode (TE mode) and to further deduce the ON/OFF amplitude ratio in the TM wave (TE wave). This also means that, throughout the article, the square signals are centered around zero, but the related time traces are vertically shifted for clarity.

4. CONCLUSION AND PERSPECTIVES

We showed that it is possible with strong cross-polarization feedback to stimulate the otherwise absent TE dynamics in a QCL. Because of the time scale in the order of hundreds of nanoseconds, we can confirm that these dynamics are not artifacts, for instance, TM–TE scattering in the optical path. Indeed, such artifacts would have a time shift related to the external cavity length, or in other words, a delay of a few nanoseconds. Furthermore, the possibility to display asymmetric patterns strengthens our claim about the absence of artifacts, because in this eventuality, the TE signal would only be a time-shifted copy of the TM signal. We believe this work opens up new challenges for theoretical analysis in QCLs, specifically in the possibility of controlling the TE emission in an intersubband device and in the role of the optothermal effects to explain microsecond

dynamics in highly damped semiconductor lasers, such as QCLs.

This work is also of interest for the development of all-optical modulation schemes that do not exist yet in the mid-infrared, at least with good performance. Modulators are indeed highly desirable in the mid-infrared domain, for high-speed transmissions, spectroscopy, and photonic reservoir computing [29]. In the case of all-optical photonics systems, experiments have already been carried out with visible and near-infrared light, but the data transmission rate can still be increased by wavelength multiplexing, thus pushing the all-optical modulators' efforts, and more generally silicon photonics integration, towards higher wavelengths [30]. The numerous nonlinear dynamics we are able to exhibit with QCLs under various optical feedback configurations [31] prove that they can be mid-infrared emitters of utter interest, and the realization of an all-optical clock diversifies the available tools for fast mid-infrared photonics.

Funding. Direction Générale de l'Armement; Agence Nationale de la Recherche (ANR-17-ASMA-0006); European Office of Aerospace Research and Development (FA9550-18-1-7001).

Acknowledgment. The authors thank Dr. Mathieu Carras for lending QCLs and acknowledge Laurédine Durupt's help for the characterization of the QWP. The authors also thank Lukas Drzewitzki for the device to compute interfaces. Portions of this work were presented at the OSA Topical Meeting on Mid-Infrared Coherent Sources (MICS), held virtually November 16–20, 2020, paper MTh3C.6 and paper MF2C.6.

Disclosures. The authors declare no conflicts of interest.

Data Availability. Data underlying the results presented in this paper are not publicly available at this time but may be obtained from the authors upon reasonable request.

REFERENCES

1. E. Rosencher and B. Vinter, *Optoelectronics* (Cambridge University, 2002).
2. R. Q. Yang, J. Xu, and M. Sweeny, "Selection rules of intersubband transitions in conduction-band quantum wells," Phys. Rev. B **50**, 7474 (1994).
3. H. Liu, M. Buchanan, and Z. Wasilewski, "How good is the polarization selection rule for intersubband transitions?" Appl. Phys. Lett. **72**, 1682–1684 (1998).
4. P. Janassek, S. Hartmann, A. Molitor, F. Michel, and W. Elsässer, "Investigations of the polarization behavior of quantum cascade lasers by Stokes parameters," Opt. Lett. **41**, 305–308 (2016).
5. D. Dhirhe, T. Slight, B. Holmes, D. Hutchings, and C. Ironside, "Quantum cascade lasers with an integrated polarization mode converter," Opt. Express **20**, 25711–25717 (2012).
6. K. Otsuka and J.-L. Chern, "High-speed picosecond pulse generation in semiconductor lasers with incoherent optical feedback," Opt. Lett. **16**, 1759–1761 (1991).
7. T. Heil, A. Uchida, P. Davis, and T. Aida, "TE-TM dynamics in a semiconductor laser subject to polarization-rotated optical feedback," Phys. Rev. A **68**, 033811 (2003).
8. Y. Takeuchi, R. Shogenji, and J. Ohtsubo, "Chaotic dynamics in semiconductor lasers subjected to polarization-rotated optical feedback," Appl. Phys. Lett. **93**, 181105 (2008).
9. G. R. Gray, D. Huang, and G. P. Agrawal, "Chaotic dynamics of semiconductor lasers with phase-conjugate feedback," Phys. Rev. A **49**, 2096 (1994).
10. G. Friart, L. Weicker, J. Danckaert, and T. Erneux, "Relaxation and square-wave oscillations in a semiconductor laser with polarization rotated optical feedback," Opt. Express **22**, 6905–6918 (2014).
11. C.-H. Uy, L. Weicker, D. Rontani, and M. Sciamanna, "Sustained oscillations accompanying polarization switching in laser dynamics," Opt. Express **26**, 16917–16924 (2018).
12. J. A. Reinoso, J. Zamora-Munt, and C. Masoller, "Extreme intensity pulses in a semiconductor laser with a short external cavity," Phys. Rev. E **87**, 062913 (2013).
13. I. Fischer, O. Hess, W. Elsässer, and E. Göbel, "High-dimensional chaotic dynamics of an external cavity semiconductor laser," Phys. Rev. Lett. **73**, 2188 (1994).
14. T. Heil, J. Mulet, I. Fischer, C. R. Mirasso, M. Peil, P. Colet, and W. Elsasser, "ON/OFF phase shift keying for chaos-encrypted communication using external-cavity semiconductor lasers," IEEE J. Quantum Electron. **38**, 1162–1170 (2002).
15. F.-Y. Lin and J.-M. Liu, "Chaotic lidar," IEEE J. Sel. Top. Quantum Electron. **10**, 991–997 (2004).
16. N. Nieubor, K. Panajotov, A. Goulet, I. Veretennicoff, and H. Thienpont, "Data transparent reconfigurable optical interconnections based on polarization-switching VCSELs and polarization-selective diffractive optical elements," IEEE Photon. Technol. Lett. **10**, 973–975 (1998).
17. T. Katayama, T. Ooi, and H. Kawaguchi, "Experimental demonstration of multi-bit optical buffer memory using 1.55 μm polarization bistable vertical-cavity surface-emitting lasers," IEEE J. Quantum Electron. **45**, 1495–1504 (2009).
18. N. Oliver, M. C. Soriano, D. W. Sukow, and I. Fischer, "Dynamics of a semiconductor laser with polarization-rotated feedback and its utilization for random bit generation," Opt. Lett. **36**, 4632–4634 (2011).
19. O. Spitz, A. Herdt, J. Wu, G. Maisons, M. Carras, C.-W. Wong, W. Elsässer, and F. Grillot, "Private communication with quantum cascade laser photonic chaos," Nat. Commun. **12**, 3327 (2021).
20. T. Li, M. Nedeljkovic, N. Hattasan, W. Cao, Z. Qu, C. G. Littlejohns, J. S. Penades, L. Mastronardi, V. Mittal, D. Benedikovic, D. J. Thomson, F. Y. Gardes, H. Wu, Z. Zhou, and G. Z. Mashanovich, "Ge-on-Si modulators operating at mid-infrared wavelengths up to 8 μm," Photon. Res. **7**, 828–836 (2019).
21. A. Evans, J. Yu, J. David, L. Doris, K. Mi, S. Slivken, and M. Razeghi, "High-temperature, high-power, continuous-wave operation of buried heterostructure quantum-cascade lasers," Appl. Phys. Lett. **84**, 314–316 (2004).
22. M. Carras, M. Garcia, X. Marcadet, O. Parillaud, A. De Rossi, and S. Bansropun, "Top grating index-coupled distributed feedback quantum cascade lasers," Appl. Phys. Lett. **93**, 011109 (2008).
23. A. Gavrielides, T. Erneux, D. W. Sukow, G. Burner, T. McLachlan, J. Miller, and J. Amonette, "Square-wave self-modulation in diode lasers with polarization-rotated optical feedback," Opt. Lett. **31**, 2006–2008 (2006).
24. C. Masoller, D. Sukow, A. Gavrielides, and M. Sciamanna, "Bifurcation to square-wave switching in orthogonally delay-coupled semiconductor lasers: theory and experiment," Phys. Rev. A **84**, 023838 (2011).
25. S. Barbieri, W. Maineult, S. S. Dhillon, C. Sirtori, J. Alton, N. Breuil, H. E. Beere, and D. A. Ritchie, "13 GHz direct modulation of terahertz quantum cascade lasers," Appl. Phys. Lett. **91**, 143510 (2007).
26. M. Dillane, B. Tykalewicz, D. Goulding, B. Garbin, S. Barland, and B. Kelleher, "Square wave excitability in quantum dot lasers under optical injection," Opt. Lett. **44**, 347–350 (2019).
27. F. Marino, G. Catalán, P. Sánchez, S. Balle, and O. Piro, "Thermo-optical 'canard orbits' and excitable limit cycles," Phys. Rev. Lett. **92**, 073901 (2004).
28. T. Aellen, R. Maulini, R. Terazzi, N. Hoyler, M. Giovannini, J. Faist, S. Blaser, and L. Hvozdara, "Direct measurement of the linewidth enhancement factor by optical heterodyning of an amplitude-modulated quantum cascade laser," Appl. Phys. Lett. **89**, 091121 (2006).
29. G. Van der Sande, D. Brunner, and M. C. Soriano, "Advances in photonic reservoir computing," Nanophotonics **6**, 561–576 (2017).
30. H. Lin, Z. Luo, T. Gu, L. C. Kimerling, K. Wada, A. Agarwal, and J. Hu, "Mid-infrared integrated photonics on silicon: a perspective," Nanophotonics **7**, 393–420 (2018).
31. O. Spitz, J. Wu, A. Herdt, G. Maisons, M. Carras, W. Elsässer, C.-W. Wong, and F. Grillot, "Extreme events in quantum cascade lasers," Adv. Photon. **2**, 066001 (2020).